Dose warping uncertainties for the accumulated rectal wall dose in cervical cancer brachytherapy

Heerden, L.E. van; Wieringen, N. van; Koedooder, K.; Rasch, C.R.N.; Pieters, B.R.; Bel, A.

ELSEVIER

CrossMark

BRACHYTHERAPY

Brachytherapy 17 (2018) 449–455

Physics

Dose warping uncertainties for the accumulated rectal wall dose in cervical cancer brachytherapy

Laura E. van Heerden*, Niek van Wieringen, Kees Koedooder, Coen R.N. Rasch, Bradley R. Pieters, Arjan Bel

Department of Radiation Oncology, Academic Medical Center/University of Amsterdam, Amsterdam, AZ The Netherlands

ABSTRACT

PURPOSE: Structure-based deformable image registration (DIR) can be used to calculate accumulated dose volume histogram parameters for cervical cancer brachytherapy (BT). The purpose of this study is to investigate dose warping uncertainties for the accumulated dose to the 2 cm^3 receiving the highest dose ($D_{2\ cm^3}$) in the rectal wall, using a physically realistic model (PRM) describing rectal wall deformation.

METHODS AND MATERIALS: For 10 patients, treated with MRI-guided pulsed dose rate BT (two times 24 × 0.75 Gy, given in two applications BT1 and BT2), the planning images were registered with structure-based DIR. The resulting transformation vectors were used to accumulate the total rectum dose from BT. To investigate the dose warping uncertainty, a PRM describing rectal deformation was used. For point pairs on $rectum_{BT1}$ and $rectum_{BT2}$ that were at the same location according to the PRM, the dose for BT1 and BT2 was added (D_{PRM}) and compared to the DIR-accumulated dose (D_{DIR}) in the BT2 point. The remaining distance after DIR between corresponding point pairs, defined as the residual distance, was calculated.

RESULTS: For points within the $D_{2\ cm^3}$ volume, more than 75% was part of the $D_{2\ cm^3}$ volume according to both PRM and DIR. The absolute dose difference was <7.3 Gy_{EQD2}, and the median (95th percentile) of the residual distance was 8.7 (22) mm.

CONCLUSIONS: DIR corresponded with the PRM for on average 75% of the $D_{2\ cm^3}$ volume. Local absolute dose differences and residual distances were large. Care should therefore be taken with DIR for dose-warping purposes in BT.

Keywords: Cervical cancer; Brachytherapy; Deformable image registration; Dose accumulation; Uncertainties

Introduction

Locally advanced cervical cancer is commonly treated with concurrent chemotherapy and radiotherapy. The radiation treatment consists of external beam radiotherapy (EBRT) combined with a brachytherapy (BT) boost in multiple applications to the tumor area. After each BT implantation, the 3D dose distribution is calculated using image-guided treatment planning. Planning aims include a recommended dose to 90% of the high-risk clinical target volume (CTV_{HR}) from EBRT and BT of 90–95 Gy_{EQD2}, expressed as equivalent dose in 2 Gy fractions (EQD_2) (1). The dose to the most irradiated 2 cm^3 of the rectum ($D_{2\ cm^3}$), which is associated with rectal toxicity, should not exceed 75 Gy_{EQD2} (2, 3).

It is recommended by the International Commission on Radiation Units and Measurements (ICRU) to assume that the high dose volumes are at the same location on the rectal wall for the evaluation of the cumulative rectum $D_{2\ cm^3}$ of multiple BT applications, meaning that the dose volume histogram (DVH) parameters can simply be added (1). With the ICRU formalism, $D_{2\ cm^3}$ is possibly overestimated, which may lead to errors in establishing the dose-response relationship in the rectum. To avoid overestimating the cumulative $D_{2\ cm^3}$, it may be preferable to sum the 3D dose distributions instead.

When summing the total dose, it is necessary to use deformable image registration (DIR) to account for rectal deformation due to differences in filling and/or the presence

Received 20 July 2017; received in revised form 13 September 2017; accepted 1 October 2017.

* Corresponding author. Department of Radiation Oncology, Academic Medical Center, University of Amsterdam, Meibergdreef 9, Amsterdam, AZ 1105, The Netherlands. Tel.: +31 (0) 20 5666896; fax: +31 (0) 20 60 91278.

E-mail address: l.e.vanheerden@amc.uva.nl (L.E. van Heerden).

1538-4721/$ - see front matter
https://doi.org/10.1016/j.brachy.2017.10.002

of air and the effect of the applicator on the position of the rectum. Earlier studies investigated the added value of DIR when calculating cumulative rectal $D_{2\ cm^3}$, and they found small differences (<10%) with direct addition of the $D_{2\ cm^3}$ (4–7). Because of the DIR-related uncertainty, they concluded that there was limited benefit of dose accumulation with DIR over direct addition of DVH parameters.

Indeed, little is known about the reliability of DIR for accumulation of the BT dose in the rectum. Jamema *et al.* analyzed uncertainties when accumulating the BT dose in the rectum, by comparing intensity-based with structure-based matching (6). They found that dose accumulation based on structure-based matching is more reliable than intensity-based matching since intensity-based DIR led to implausible deformation and a systematic underestimation of the dose. Dose accumulation accuracy may improve further when the matching is performed based on a physically realistic model (PRM) that includes an estimate of the biomechanical properties because such properties are not taken into account in the structure-based DIR. As of yet, no studies have investigated the dose warping uncertainties for accumulated BT doses through landmark identification. Such anatomical landmarks cannot be identified through visual assessment on BT planning images (CT/anatomical MRI). We propose to investigate the uncertainties for dose accumulation based on structure-based matching by identifying corresponding point pairs on the rectum wall using a model describing rectal deformation.

The purpose of this study is therefore to accumulate the total BT dose to the rectal wall using structure-based DIR and to investigate dose warping uncertainties using a PRM describing rectal deformation.

Methods and materials

Patients

Ten cervical cancer patients treated with EBRT (45–50 Gy in 1.8–2.0 Gy/fraction) and a pulsed dose rate BT boost, delivered in two applications BT1 and BT2 of 18 Gy each in pulse doses of 75 cGy every hour, were included in this study. EBRT was planned with volumetric modulated arc therapy. For BT, an intrauterine device with ovoids and if needed interstitial needles were used. The interval between the BT applications was <2 weeks. The planning aim was a cumulative D_{90} of 90–95 Gy_{EQD2} from EBRT and BT on the CTV_{HR}. To spare the rectum, the planned cumulative $D_{2\ cm^3}$ from EBRT and the BT applications should not exceed 75 Gy_{EQD2}. Prior to the BT delivery, T_2-weighted Turbo Spin Echo MRI (voxel size: 0.5 × 0.5 × 3.3 mm^3) was acquired on an Ingenia 3T MRI scanner (Philips Healthcare, Best, The Netherlands) (8). On the MRI scans, the rectum was delineated from the rectosigmoid junction to the level of the anal sphincter. Rectum volumes at the time of BT1 and BT2 are described in Supplementary Table 1. BT planning was performed using Oncentra Brachy 4.5 (Elekta, Veenendaal, The Netherlands), using a library for applicator reconstruction, after which the plan was manually optimized. Typical dose distributions are shown in Fig. 1.

Implementation of the PRM

We used a PRM describing rectal deformation to localize corresponding point pairs on the rectum wall because there is a lack of corresponding anatomical landmarks that can be distinguished on the BT planning MRI (9, 10). The principles of the PRM were previously described by Meijer *et al.* (11) and Hoogeman *et al.* (12). This model was already used to quantify rectum displacements (12, 13) and to relate dose surface maps to toxicity (14, 15).

The model is based on physiological characteristics of the rectum (11, 12, 16). The rectum is attached on the dorsal side to the sacrum by the mesorectum. The rectum wall has an inner lining of circular smooth muscle which will stretch and elongate with increased rectal filling. This stretching, which is assumed to always be perpendicular to the central axis is accompanied by an overall narrowing of the rectum wall. Due to this trade-off between rectal wall thickness and stretching of the rectum muscularis, the amount of tissue in the rectal wall is constant in every intersection perpendicular to the central axis. Since displacements along the length of the axis can be neglected, the central axes of the rectum of BT1 and BT2 ($rectum_{BT1}$, $rectum_{BT2}$) are assumed to be fixed in length.

The central axes were constructed using a minimum distance field as described by Zhou *et al.* (17), to find for each lateral plane the voxel with the shortest distance to the boundary (Matlab R2014b, Mathworks Inc., MA) (Fig. 2). Subsequently, the axis was smoothed using a moving average filter with a span of 0.5 cm.

For both $rectum_{BT1}$ and $rectum_{BT2}$, orthogonal planes were constructed at five evenly spaced positions on the axis. For areas of high curvature in the rectum, the planes might intersect. To avoid intersecting planes, only five planes were constructed, and the planes were rotated away from each other if the local curvature of the central axes exceeded a fixed maximum. Next, 100 points were evenly distributed over the intersection curve of each plane with the rectal wall. It was assumed that the rectum is fixed at the dorsal side. This fixed dorsal point was point 1, and it was found by sampling the point on the intersection curve for which the left-right coordinate was closest to that of the central axis. All corresponding point pairs were stored to be used for the DIR evaluation.

DIR and dose accumulation

The dose from BT1 and BT2 was accumulated in EQD_2 using DIR to take into account rectal deformation. First, the BT doses were converted to EQD_2 on a voxel-by-voxel level using LQ-model based equations with an α/β value

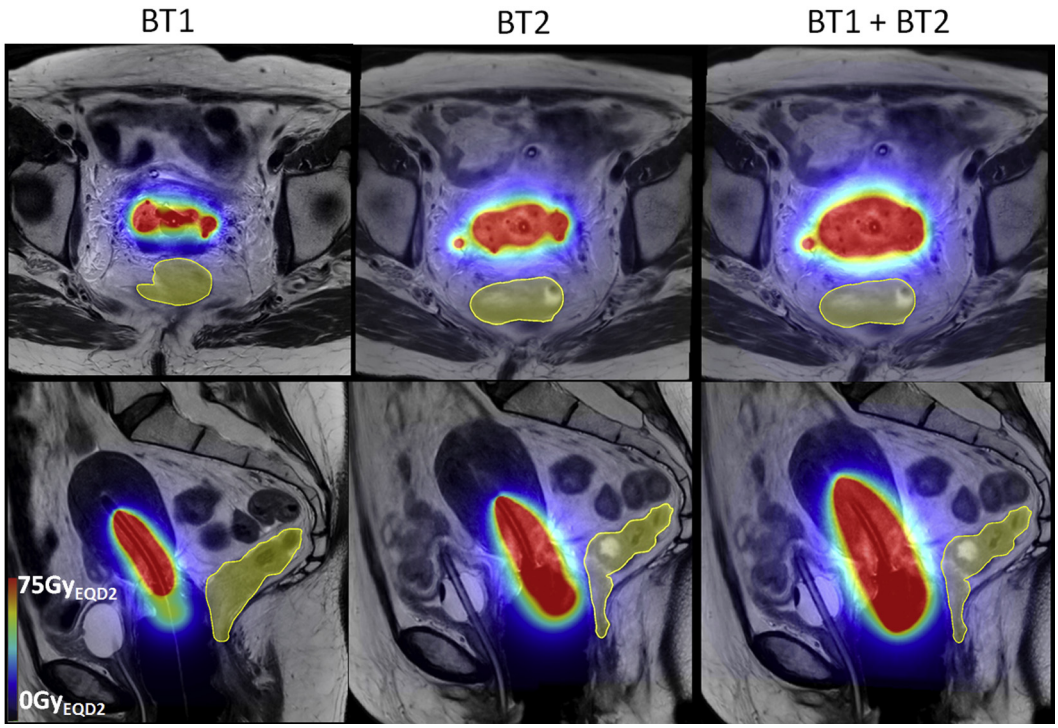

Fig. 1. Axial (top row) and sagittal view (bottom row) of the patient MRI with a color wash of the planned dose from BT1 (left), BT2 (middle), and the dose from BT1 and BT2, accumulated using structure-based deformable image registration as described in this paper (right). The rectum is shown in yellow. (For interpretation of the references to color in this figure legend, the reader is referred to the Web version of this article.)

of 3 Gy for late rectal toxicity and a 1.5-hour repair half-time (1, 18).

The feature-based deformable registration (FBDR) tool, available in a research version of Oncentra Brachy was used for structure-based DIR with the BT1 as the reference frame. The DIR algorithm in the FBDR tool is directly derived from the symmetric unidirectional thin plate spline robust point matching algorithm (10, 19, 20). The delineated rectums were converted to three-dimensional surface meshes, and a mapping was established to propagate elements on the surface of rectum_{BT1} to the surface of rectum_{BT2}.

To evaluate the DIR accuracy, the Dice coefficient (21) was calculated between the propagated (BT1) and reference (BT2) contours as well the mean surface distance error, which is the Euclidean distance between the reference and propagated contours. Finally, the transformation vectors were used to deform the BT1 dose distribution, and the BT1 and BT2 doses were summed voxel-by-voxel (Fig. 1, right panel).

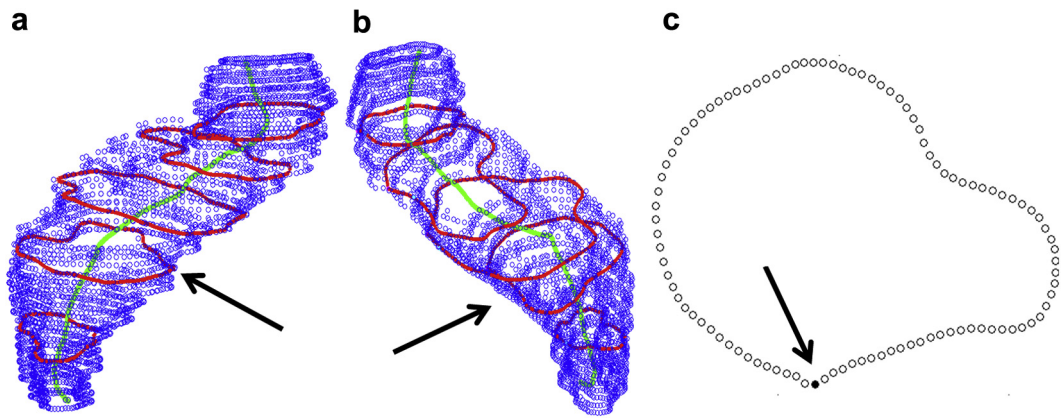

Fig. 2. View from the left side (a) and the right side (b) of the rectum point cloud (blue), with the central axis (green) and the five intersection curves describing the planes orthogonal to the central axis (red). (c) The curve indicated by the arrows (in a and b) is represented. One hundred points were evenly distributed over the curve. The filled dot and arrow indicates the most dorsal point. (For interpretation of the references to color in this figure legend, the reader is referred to the Web version of this article.)

DIR accuracy in the rectal wall

The point pairs defined with the PRM were used to quantify uncertainties in the accumulated DIR dose. For corresponding points on $rectum_{BT1}$ and $rectum_{BT2}$, the dose of BT1 and BT2 was added (D_{PRM}) and compared to the DIR-accumulated dose (D_{DIR}) in the BT2 point. In addition, the remaining distance after DIR between corresponding points, which is defined as the residual distance, was calculated (Fig. 3).

For BT, the high dose regions in the rectum are most relevant. Therefore, only those point pairs for which D_{DIR} was $\geq D^{ICRU}_{2\ cm^3}$ were considered in the rest of the analysis. The $D^{ICRU}_{2\ cm^3}$ was calculated by adding $D_{2\ cm^3}$ from BT1 to $D_{2\ cm^3}$ from BT2, according to the ICRU formalism. $D^{ICRU}_{2\ cm^3}$ was used as a threshold because this is a conservative estimate of the cumulative $D_{2\ cm^3}$ since it assumes the high dose volumes are overlapping. The analysis was done in this way to avoid analyzing points outside the $D_{2\ cm^3}$ volume.

We calculated the average D_{PRM} and D_{DIR} for all patients and compared these values. For every patient, the 25th, 50th, 75th, and 95th percentiles of the absolute dose difference ($|D_{DIR}-D_{PRM}|$) and the 25th, 50th, 75th, and 95th percentiles of the residual distance were calculated. For both the absolute dose difference and residual distance, the 50th and 95th percentile over all patients was determined.

Points within the 2 cm^3 volume receiving the highest dose should be correctly identified, meaning that DIR is in agreement with PRM about which points are part of the $D_{2\ cm^3}$ volume. For the points under consideration, this was investigated by calculating the average percentage for which $D_{PRM} \geq D^{ICRU}_{2\ cm^3}$ over all patients.

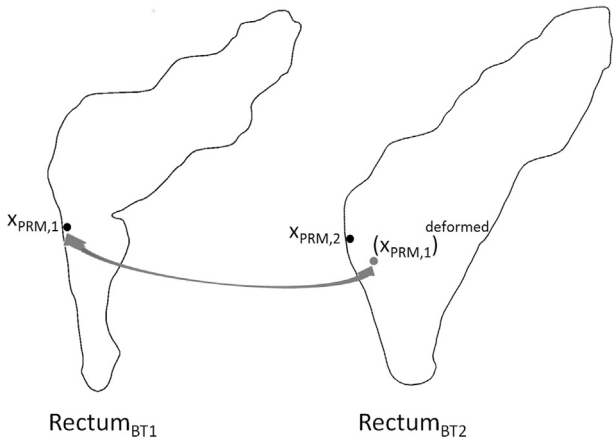

Fig. 3. Corresponding point pair on the rectum of BT1 and BT2 ($x_{PRM,1}$ and $x_{PRM,2}$) is localized using the PRM. For this point pair, D_{PRM} and D_{DIR} are calculated according to: $D_{PRM} = D_{BT1}(x_{PRM,1}) + D_{BT2}(x_{PRM,2})$ and $D_{DIR} = D^{deformed}_{BT1}(x_{PRM,2}) + D_{BT2}(x_{PRM,2})$. The dose difference is $D_{PRM} - D_{DIR}$. The residual distance (RD) is the Euclidean distance between $x_{PRM,2}$ and the deformed point $x_{PRM,1}$: $RD = |x^{deformed}_{PRM,1} - x_{PRM,2}|$.

Results

The Dice coefficient after DIR was between 0.95 and 0.97, and the mean surface distance error was between 0.2 and 0.7 mm, showing that after DIR, the rectum contours were overlapping. Over all patients, on average 11% of the PRM points were within the volume for which D_{DIR} was $\geq D^{ICRU}_{2\ cm^3}$, and the mean (range) of the number of points was 56 (22–81). Only these point pairs are considered in the following results.

Averaged over all patients, the mean D_{PRM} was 1.3 Gy_{EQD2} higher than the mean D_{DIR}, with differences ranging between (−3.5) and 4.9 Gy_{EQD2}. For 9 out of 10 patients, the mean D_{PRM} was smaller than the mean D_{DIR}.

For the median absolute dose difference, values varied over all patients between 0.6 and 4.9 Gy_{EQD2}, while the 95th percentile varied between 1.4 and 7.3 Gy_{EQD2} (Fig. 4). For all patients combined, 50% of the absolute dose differences were <2.2 Gy_{EQD2}, and 95% of the absolute dose differences was <5.8 Gy_{EQD2}. The residual distance varied between 1.5 and 33 mm (Fig. 5). For all calculated residual distance values, 50% was <8.7 mm and 95% was <23 mm. D_{PRM} was $\geq D^{ICRU}_{2\ cm^3}$ for 75% of the points under consideration, meaning that DIR and PRM were in agreement that these points were part of the $D_{2\ cm^3}$ volume.

Discussion

This is the first study to use a PRM that describes rectal deformation to investigate local dose warping uncertainties for the BT rectum dose accumulated with structure-based DIR. We used the PRM to locate points on the rectal wall. For points within the 2 cm^3 receiving the highest dose, dose differences could be as high 7.3 Gy_{EQD2}, and the median

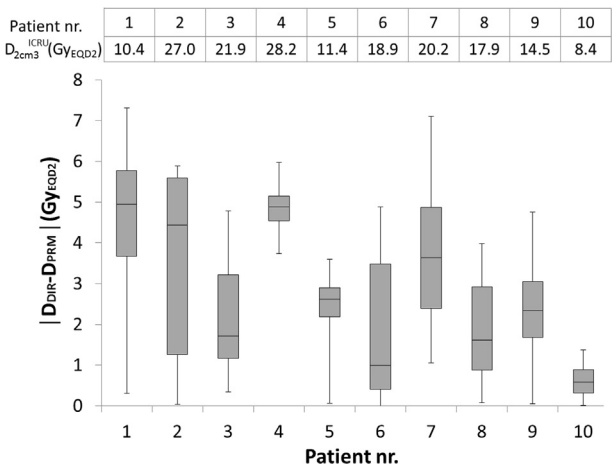

Fig. 4. Boxplot of the absolute dose difference calculated for corresponding points within the $D_{2\ cm^3}$ volume for all patients, with the median and the 25th and 75th percentiles. The whiskers show the minimum and the 95th percentile. The table shows the $D^{ICRU}_{2\ cm^3}$, which is the cumulative $D_{2\ cm^3}$ of both applications, calculated with the ICRU formalism.

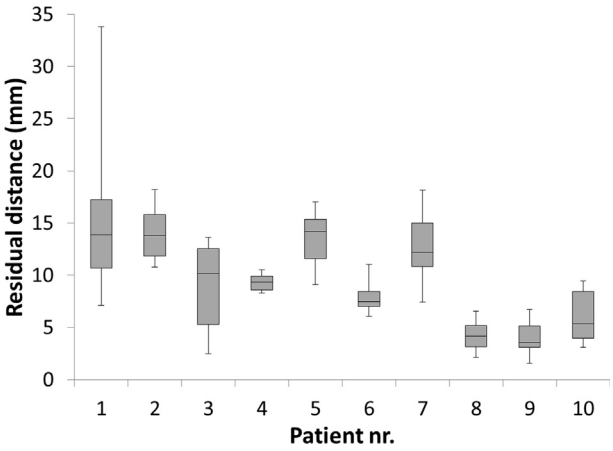

Fig. 5. Boxplot of the residual distance after DIR between corresponding points within the $D_{2\ cm^3}$ volume for all patients, with the median and the 25th and 75th percentile. The whiskers show the minimum and the 95th percentile.

residual distance after DIR was 8.7 mm. For the points under consideration, more than 75% was part of the $D_{2\ cm^3}$ volume according to both PRM and DIR. Our results show that due to large local uncertainties dose accumulation with this structure-based DIR algorithm is problematic for doses that have steep gradients such as in BT.

There are many uncertainties related to cervical cancer BT (22, 23). Interfraction and intrafraction motion and delineation uncertainties are major contributors to the total uncertainty in estimation of the delivered dose (24, 25). Calculation of accumulated dose from BT using the ICRU formalism is another source of uncertainty, since it may lead to a systematic overestimation of the delivered dose. However, using DIR to calculate cumulative DVH parameters will introduce large new uncertainties, as shown in results section.

Structure-based DIR was used in this study to accumulate BT dose in the rectum. The choice of DIR algorithm is important because the quality of the registration depends strongly on the DIR performance. According to Jamema *et al.* (6), who compared structure-based and intensity-based DIR for 3D accumulated $D_{2\ cm^3}$, structure-based DIR is the best choice for DIR-based dose accumulation in the rectum. Compared to earlier studies, (5, 7) high Dice coefficients (>0.95) and low mean residual distances (<0.7 mm) were achieved in this study with structure-based DIR, showing that the rectum contours were matched with high accuracy.

We narrowed down our results to the dose difference and residual distance of only those point pairs for which D_{PRM} was $\geq D^{ICRU}_{2\ cm^3}$ because DVH parameters of the high dose volumes are commonly reported for rectum in BT. Although 500 points were sampled at different positions on the rectal wall, only a small selection (11%) was relevant for this study. These points were predominantly located at the more caudal region of the rectum, which is near the region of the BT boost. Because points were localized in planes over the entire rectal surface, the method explained in this study could be used to evaluate accumulated doses for different dose schemes, such as fractionated EBRT, by including more points. However, this was beyond the scope of this study.

For the points under consideration, the mean D_{DIR} was on average 1.3 Gy_{EQD2} higher than the mean D_{PRM}. This is as expected because the high dose area obtained by PRM might not be the same as obtained by DIR. For one patient, PRM overestimated the mean dose to the $D_{2\ cm^3}$ volume. For this patient, the true minimum within the volume was possibly not found because only 22 points were included in the analysis.

The absolute dose difference for individual points could be as high as 7.3 Gy_{EQD2}, whereas the median absolute dose difference over all patients was 2.2 Gy_{EQD2}, and the 95th percentile of the residual distance was 23 mm. This shows that locally uncertainties can be large. The impact of these uncertainties on the $D_{2\ cm^3}$ is unclear. This could be evaluated by calculating $D_{2\ cm^3}$ using the PRM and then compare this to $D_{2\ cm^3}$ calculated with DIR, but this is not possible with the method used in this study. About 75% of the points were identified as part of the $D_{2\ cm^3}$ volume by both PRM and DIR, meaning that the points were merely redistributed by DIR within the $D_{2\ cm^3}$ volume. Thus, the location of the $D_{2\ cm^3}$ volume in the DIR accumulated dose is similar to the location of the $D_{2\ cm^3}$ volume in the real dose.

For patient 1, the 95th percentile of the residual distance was as high as 33 mm. Visual inspection showed that a high overlap of the rectum contours was achieved near the high dose area (Fig. 6). However, this was the patient with the largest absolute (48 cm^3) and relative volume difference (volume BT2/volume BT1: 2.09) between rectum 1 and rectum 2 (see Supplementary Table 1). This indicates a large difference in rectal filling, which might have affected the quality of the registration.

There are no other studies which investigate BT dose uncertainties in the rectum in corresponding point pairs on the rectum wall; therefore, it is not possible to directly compare the dose uncertainties we found. For the residual distance, Nassef *et al.* (26) investigated uncertainties in accumulated rectum dose from EBRT using the daily CBCTs, for prostate cancer. In a numerical phantom of the female pelvis, they defined surface points on the rectum and found mean landmark errors of 2.4 mm on the rectal wall. Vasquez-Osorio *et al.* (10) defined landmarks near the cervix uterus, bladder, and in the mesorectum and reported the mean error (3.4 mm) of all these landmarks for MRI registration using the same DIR algorithm as this study. These values were smaller than the median residual distance of 8.7 mm found in this study. However, in the mentioned studies, landmarks over the whole rectum or near the rectum were included, as well as landmarks near other structures, whereas in our study, we evaluated only points in the $D_{2\ cm^3}$ volume of the rectum.

The evaluated points were all located on the rectal surface, whereas the $D_{2\ cm^3}$ volume could partly be filling.

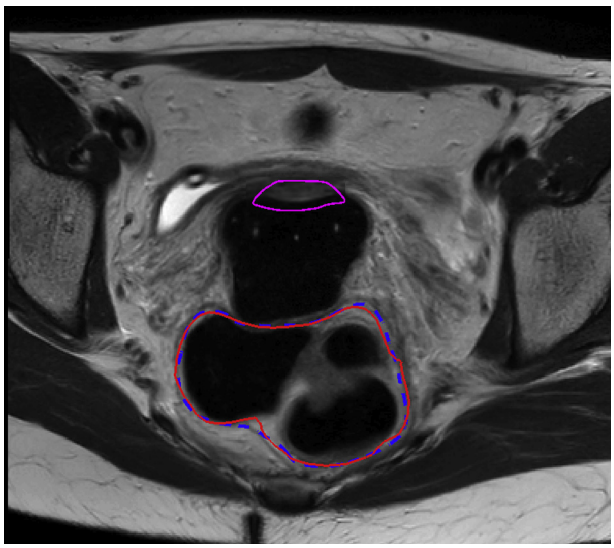

Fig. 6. Axial view of the BT MRI of patient 1, where the propagated rectum contour (solid) is shown together with the reference contour (dashed). The contours are shown close to the target (magenta). (For interpretation of the references to color in this figure legend, the reader is referred to the Web version of this article.)

According to Wachter-Gerstner *et al.* (27) and Olszewska *et al.* (28), the $D_{2\ cm^3}$ calculated from the DVH of the external contour is a good estimate of rectal wall dose. Thus, our method is adequate to determine dose errors in the $D_{2\ cm^3}$ volume.

In this study, we did not investigate dose warping uncertainties for EBRT-BT dose accumulation. Residual distances between registered EBRT and BT rectums will likely be comparable to the BT-BT registrations reported in this study, since in our institute for EBRT and BT the same pretreatment instructions apply to control the rectal filling and therefore the rectal volumes will be similar. Yet, although geometrical errors will be large, dose errors for EBRT-to-BT accumulation will be small for the patients included in this study. For EBRT, a planning aim was used for the rectum ($D_{1\ cm^3} < 103\%$ of the prescription dose) to ensure a uniform dose. We focused on errors for the BT-to-BT dose accumulation because the BT dose has high gradients and voxel-to-voxel correspondence of DIR is more important for a nonuniform dose. An extensive DIR analysis of the local errors in EBRT-to-BT accumulation would be interesting when more conformal EBRT planning strategies with smaller margins are used.

The PRM includes assumptions based on physiological characteristics of the rectum. However plausible these assumptions, a limitation of this study is that the PRM was not validated for point-to-point consistency. We could not identify anatomical points on the rectum wall on the planning MRI to check the model. It could be argued that for points located on the caudal side of the rectum, the point-to-point consistency is worse than for dorsal points. In the model, we assume isotropic expansion away from the most dorsal point. For caudally located point pairs, the position will be more affected by local non-isotropic expansions of the rectum, such as gas bubbles.

An earlier study by Meijer *et al.* showed that EBRT DVHs of the rectal wall constructed using the PRM and of the delineated rectal wall were comparable. Future work should look into such an analysis of the PRM validity using visible landmarks as has already been done for DIR in the bladder (29). Other future studies could accumulate the total BT dose to the rectal wall using the PRM and compare accumulated DVH parameters to the direct addition method.

Conclusions

For a large part (75%) of the $D_{2\ cm^3}$ volume, DIR corresponded with PRM. Within the $D_{2\ cm^3}$ volume, absolute dose differences were large (<7.3 Gy_{EQD2}), as well as the median residual distance (8.7 mm). Care should therefore be taken for dose accumulation with this DIR algorithm for doses that have steep gradients such as in BT.

Acknowledgments

The authors are grateful to Dr Joost Schillings from Elekta Brachytherapy for his help with the FBDR tool.

Funding: This work was funded by Elekta Brachytherapy (II 250008).

Disclosure of conflict of interest: A.B. is involved in several projects funded by Elekta.

Supplementary data

Supplementary data related to this article can be found at https://doi.org/10.1016/j.brachy.2017.10.002.

References

[1] Pötter R, Haie-Meder C, Van Limbergen E, *et al*. Recommendations from gynaecological (GYN) GEC ESTRO working group (II): Concepts and terms in 3D image-based treatment planning in cervix cancer brachytherapy-3D dose volume parameters and aspects of 3D image-based anatomy, radiation physics, radiobiology. *Radiother Oncol* 2006;78:67–77.

[2] Georg P, Pötter R, Georg D, *et al*. Dose effect relationship for late side effects of the rectum and urinary bladder in magnetic resonance image-guided adaptive cervix cancer brachytherapy. *Int J Radiat Oncol Biol Phys* 2012;82:653–657.

[3] Mazeron R, Fokdal LU, Kirchheiner K, *et al*. Dose–volume effect relationships for late rectal morbidity in patients treated with chemoradiation and MRI-guided adaptive brachytherapy for locally advanced cervical cancer: Results from the prospective multicenter EMBRACE study. *Radiother Oncol* 2016;120:412–419.

[4] Abe T, Tamaki T, Makino S, *et al*. Assessing cumulative dose distributions in combined radiotherapy for cervical cancer using deformable image registration with pre-imaging preparations. *Radiat Oncol* 2014;9:293.

[5] Flower E, Do V, Sykes J, *et al*. Deformable image registration for cervical cancer brachytherapy dose accumulation: Organ at risk

dose–volume histogram parameter reproducibility and anatomic position stability. *Brachytherapy* 2017;16:387–392.
[6] Jamema SV, Mahantshetty U, Andersen E, *et al*. Uncertainties of deformable image registration for dose accumulation of high-dose regions in bladder and rectum in locally advanced cervical cancer. *Brachytherapy* 2015;15:953–962.
[7] Sabater S, Andres I, Sevillano M, *et al*. Dose accumulation during vaginal cuff brachytherapy based on rigid/deformable registration vs. single plan addition. *Brachytherapy* 2014;13:343–351.
[8] van Heerden LE, Gurney-Champion OJ, van Kesteren Z, *et al*. Quantification of image distortions on the Utrecht interstitial CT/MR brachytherapy applicator at 3T MRI. *Brachytherapy* 2016;15:118–126.
[9] Torkzad MR, Påhlman L, Glimelius B. Magnetic resonance imaging (MRI) in rectal cancer: A comprehensive review. *Insights Imaging* 2010;1:245–267.
[10] Vásquez Osorio EM, Kolkman-Deurloo I-KK, Schuring-Pereira M, *et al*. Improving anatomical mapping of complexly deformed anatomy for external beam radiotherapy and brachytherapy dose accumulation in cervical cancer. *Med Phys* 2015;42:206–220.
[11] Meijer GJ, van den Brink M, Hoogeman MS, *et al*. Dose–wall histograms and normalized dose–surface histograms for the rectum: A new method to analyze the dose distribution over the rectum in conformal radiotherapy. *Int J Radiat Oncol* 1999;45:1073–1080.
[12] Hoogeman MS, van Herk M, de Bois J, *et al*. Quantification of local rectal wall displacements by virtual rectum unfolding. *Radiother Oncol* 2004;70:21–30.
[13] Nijkamp J, Pos FJ, Nuver TT, *et al*. Adaptive radiotherapy for prostate cancer using kilovoltage cone-beam computed tomography: First clinical results. *Int J Radiat Oncol* 2008;70:75–82.
[14] Heemsbergen WD, Hoogeman MS, Hart GAM, *et al*. Gastrointestinal toxicity and its relation to dose distributions in the anorectal region of prostate cancer patients treated with radiotherapy. *Int J Radiat Oncol* 2005;61:1011–1018.
[15] Wortel RC, Witte MG, van der Heide UA, *et al*. Dose–surface maps identifying local dose–effects for acute gastrointestinal toxicity after radiotherapy for prostate cancer. *Radiother Oncol* 2015;117:515–520.
[16] Baxter NN, Burnstein MJ. Treatment of Colorectal Cancer. *Surg Oncol Clin N Am* 2014;23:11–12.
[17] Zhou SM, Marks LB, Tracton GS, *et al*. A new three-dimensional dose distribution reduction scheme for tubular organs. *Med Phys* 2000;27:1727–1731.
[18] International Commission of Radiation and Units. ICRU report 89. *J ICRU* 2013;13:1–2.
[19] Bondar L, Hoogeman M, Mens JW, *et al*. Toward an individualized target motion management for IMRT of cervical cancer based on model-predicted cervix-uterus shape and position. *Radiother Oncol* 2011;99:240–245.
[20] Vasquez Osorio EM, Hoogeman MS, Bondar L, *et al*. A novel flexible framework with automatic feature correspondence optimization for nonrigid registration in radiotherapy. *Med Phys* 2009;36:2848–2859.
[21] Dice LR. Measures of the amount of ecologic association between species. *Ecology* 1945;26:297–302.
[22] Kirisits C, Rivard MJ, Baltas D, *et al*. Review of clinical brachytherapy uncertainties: Analysis guidelines of GEC-ESTRO and the AAPM. *Radiother Oncol* 2014;110:199–212.
[23] Nesvacil N, Tanderup K, Lindegaard JC, *et al*. Can reduction of uncertainties in cervix cancer brachytherapy potentially improve clinical outcome? *Radiother Oncol* 2016;120:390–396.
[24] Hellebust TP, Tanderup K, Lervåg C, *et al*. Dosimetric impact of interobserver variability in MRI-based delineation for cervical cancer brachytherapy. *Radiother Oncol* 2013;107:13–19.
[25] Nesvacil N, Tanderup K, Hellebust TP, *et al*. A multicentre comparison of the dosimetric impact of inter- and intra-fractional anatomical variations in fractionated cervix cancer brachytherapy. *Radiother Oncol* 2013;107:20–25.
[26] Nassef M, Simon A, Cazoulat G, *et al*. Quantification of dose uncertainties in cumulated dose estimation compared to planned dose in prostate IMRT. *Radiother Oncol* 2016;119:129–136.
[27] Wachter-Gerstner N, Wachter S, Reinstadler E, *et al*. Bladder and rectum dose defined from MRI based treatment planning for cervix cancer brachytherapy: Comparison of dose-volume histograms for organ contours and organ wall, comparison with ICRU rectum and bladder reference point. *Radiother Oncol* 2003;68:269–276.
[28] Olszewska AM, Saarnak AE, de Boer RW, *et al*. Comparison of dose-volume histograms and dose-wall histograms of the rectum of patients treated with intracavitary brachytherapy. *Radiother Oncol* 2001;61:83–85.
[29] Wognum S, Heethuis SE, Rosario T, *et al*. Validation of deformable image registration algorithms on CT images of ex vivo porcine bladders with fiducial markers. *Med Phys* 2014;41:71916.